NAVAL POSTGRADUATE SCHOOL

MONTEREY, CALIFORNIA

THESIS

MODELING ATOM INTERFEROMETRY USING WIGNER DISTRIBUTIONS

by

Jon R. Campau

June 2021

Thesis Advisor:	Francesco A. Narducci
Second Reader:	Fabio D. Durante Pereira Alves

THIS PAGE INTENTIONALLY LEFT BLANK

REPORT DOCUMENTATION PAGE			*Form Approved OMB No. 0704-0188*

1. AGENCY USE ONLY *(Leave blank)*	**2. REPORT DATE** June 2021	**3. REPORT TYPE AND DATES COVERED** Master's thesis

4. TITLE AND SUBTITLE MODELING ATOM INTERFEROMETRY USING WIGNER DISTRIBUTIONS	**5. FUNDING NUMBERS**
6. AUTHOR(S) Jon R. Campau	
7. PERFORMING ORGANIZATION NAME(S) AND ADDRESS(ES) Naval Postgraduate School Monterey, CA 93943-5000	**8. PERFORMING ORGANIZATION REPORT NUMBER**
9. SPONSORING / MONITORING AGENCY NAME(S) AND ADDRESS(ES) N/A	**10. SPONSORING / MONITORING AGENCY REPORT NUMBER**

11. SUPPLEMENTARY NOTES The views expressed in this thesis are those of the author and do not reflect the official policy or position of the Department of Defense or the U.S. Government.

12a. DISTRIBUTION / AVAILABILITY STATEMENT Approved for public release. Distribution is unlimited.	**12b. DISTRIBUTION CODE** A

13. ABSTRACT (maximum 200 words)

The Navy is interested in obtaining alternate methods of navigation for Global Positioning System (GPS) denied environments, and one candidate is precision inertial navigation using atom interferometers. A good method of modeling the behavior of a group of atoms in an interferometer is to use the Wigner distribution. In atom interferometry, the distribution of a set of atoms starts with a well-defined distribution in position and momentum space (usually Gaussian), but their positions spread more rapidly than their momenta, forming an ellipse in phase (Wigner) space. However, this ellipse can rotate as it propagates, revealing new quantum phenomena. This project models the behavior of an atom in an interferometer and investigates the underlying physics of the Wigner ellipse rotation. Although no discoveries were made, the Wigner phase space model succinctly communicates the dynamics of the atoms inside the interferometer.

14. SUBJECT TERMS atom interferometry, gyroscopes, accelerometers, inertial navigation, Wigner distributions, Weyl transforms	**15. NUMBER OF PAGES** 47
	16. PRICE CODE

17. SECURITY CLASSIFICATION OF REPORT	**18. SECURITY CLASSIFICATION OF THIS PAGE**	**19. SECURITY CLASSIFICATION OF ABSTRACT**	**20. LIMITATION OF ABSTRACT**
Unclassified	Unclassified	Unclassified	UU

NSN 7540-01-280-5500

Standard Form 298 (Rev. 2-89)
Prescribed by ANSI Std. 239-18

THIS PAGE INTENTIONALLY LEFT BLANK

Approved for public release. Distribution is unlimited.

MODELING ATOM INTERFEROMETRY USING WIGNER DISTRIBUTIONS

Jon R. Campau
Ensign, United States Navy
BS, United States Naval Academy, 2020

Submitted in partial fulfillment of the
requirements for the degree of

MASTER OF SCIENCE IN PHYSICS

from the

NAVAL POSTGRADUATE SCHOOL
June 2021

Approved by: Francesco A. Narducci
Advisor

Fabio D. Durante Pereira Alves
Second Reader

Kevin B. Smith
Chair, Department of Physics

THIS PAGE INTENTIONALLY LEFT BLANK

ABSTRACT

The Navy is interested in obtaining alternate methods of navigation for Global Positioning System (GPS) denied environments, and one candidate is precision inertial navigation using atom interferometers. A good method of modeling the behavior of a group of atoms in an interferometer is to use the Wigner distribution. In atom interferometry, the distribution of a set of atoms starts with a well-defined distribution in position and momentum space (usually Gaussian), but their positions spread more rapidly than their momenta, forming an ellipse in phase (Wigner) space. However, this ellipse can rotate as it propagates, revealing new quantum phenomena. This project models the behavior of an atom in an interferometer and investigates the underlying physics of the Wigner ellipse rotation. Although no discoveries were made, the Wigner phase space model succinctly communicates the dynamics of the atoms inside the interferometer.

THIS PAGE INTENTIONALLY LEFT BLANK

Table of Contents

THIS PAGE INTENTIONALLY LEFT BLANK

List of Figures

CHAPTER 1:
Atom Interferometry

Before quantum mechanics was discovered, Albert Michelson used an optical interferometer in an attempt to measure the ether, the supposed medium through which light travels, now known to be fictitious. Although he was unsuccessful in finding the ether, the technology of optical interferometers, which measure small length differences in two nearly identical photon beam paths, has been an important part of optical research ever since. Different designs and configurations of these devices are used in a variety of wide ranging applications, including Ring Laser Gyroscopes (RLGs) for rotation sensing [2]. Atom interferometry is a promising and relatively new method of applying the fundamentals of interferometers that incorporates the quantum wave mechanics of particles. Instead of photons, atoms are the particles that take two different paths and recombine. Now light and matter have swapped roles: matter (e.g. glass) splits, redirects, and recombines light in an optical interferometer, but light splits, redirects, and recombines matter in an atom interferometer.

In the simulations conducted in this paper, great effort was expended to show that the atoms end up in exactly the same state at the end of the interferometer regardless of the path taken. However, we note that if there was any change or inconsistency in an external field (gravity, electric, magnetic) then the two paths would not be equivalent, but have a phase difference. The interferometer construction allows very small phase difference to be detected quite easily. The primary potential naval application is inertial navigation, which allows a ship to accurately navigate without GPS. Usually this is done by starting with the ship in a known position with a steady course and speed. Any subsequent acceleration or course rotation will show up as a phase difference in an interferometer. These phase differences measure the amount of acceleration (whether a change in course or speed) and this change can be factored in to determine the current position of the ship given its prior position. Interferometers can also assist navigation using magnetic fields. This can happen because the Earth's magnetic field is not precisely uniform throughout its surface, and therefore the detection of these local variations can help identify where on the Earth a particular ship is without needing to wait for GPS to come back on or night to fall for a celestial fix. Detecting small gravitational changes could also be valuable: holes and tunnels could be more easily

found with an atom interferometer.

1.1 Physics of a Two Level Atom

To understand the physics of an interferometer, it is important to review the basics of a two level atom. As the name would indicate, the example atom has two states that we label $|0\rangle$ and $|1\rangle$, separated by an energy $E = \hbar\omega_0$, where ω_0 is the frequency of the photon associated with the transition and $\hbar$ is the reduced Planck's constant. Whenever the atom jumps between the two states, it either absorbs energy E to move from $|0\rangle$ to $|1\rangle$ or releases energy E as it moves from $|1\rangle$ to $|0\rangle$. Energy transitions in two level atoms are often mediated by the atomic dipole transition moment d. If we let $\kappa = \frac{2d}{\hbar}$ and $\mathcal{E}$ be the electric field amplitude, we note that the product $\kappa\mathcal{E}$ has units of frequency. The electric field of the laser causing the transition can be modeled by

$$E(z,t) = \mathcal{E}e^{i(kz-\omega_L t+\phi)} + c.c. \tag{1.1}$$

When the laser is exactly on resonance, or $\omega_L = \omega_0$, then the two level atom oscillates between $|0\rangle$ and $|1\rangle$ at a frequency known as the resonant Rabi frequency, defined as $\Omega_0 = \kappa\mathcal{E}$ [3].

Additionally, it is helpful to define the quantity

$$\theta(t) = \int_0^t \kappa E(t')dt', \tag{1.2}$$

where $\theta(t)$ is a phase angle representing the pulse area. In the case of a laser illuminating a two level atom with a constant electric field $\mathcal{E}_0$ from time t_1 to t_2, then the pulse area is

$$\theta(t) = \Omega_0(t_2 - t_1). \tag{1.3}$$

If the atom is initially in the ground state, then the state of the system at time t is given by [4]

$$|\Psi(t)\rangle = \cos\theta(t)/2\,|0\rangle + \sin\theta(t)/2\,|1\rangle\,. \tag{1.4}$$

From Equations 1.2, 1.3, and 1.4, it is evident that θ regulates the state of the atom when it interacts with a resonant laser field. The important physical interpretation is that the duration of a laser pulse determines the atom population that transfers from one state to another. When θ is an odd multiple of π, then the atom always switches states, but if θ is an even multiple of π, then the atom cycles through another state and returns to the original state (Equation 1.4). In atom interferometry, as with all other quantum optics applications, the laser must have the correct photon energy and pulse length in order to ensure the desired interaction. The relevant pulses for this paper are the so called π pulse and the $\frac{\pi}{2}$ pulse. As can be inferred from Equation 1.4 above, the π pulse completely inverts the state of the atom, guaranteeing a state change from excited to ground or ground to excited. The $\frac{\pi}{2}$ pulse changes the state with a probability of $\frac{1}{2}$, which means that a two level atom initially in state $\psi = |0\rangle$ will be in a state of coherent superposition $\psi = \frac{1}{\sqrt{2}}(|0\rangle + |1\rangle)$ after the pulse.

1.2 Introduction to Atom Interferometry

Atom interferometry is a process analogous to optical interferometry: both involve a beam of particles that splits in two nearly identical trajectories and then recombine. Beams of light travel down two separated paths in optical interferometers. Analogously, atom interferometers excite groups of cold atoms with laser pulses in order to create two different paths in real space and phase space [5]. In a Mach-Zender configuration, a group of atoms is prepared in a ground state, then stimulated by three consecutive laser pulses that cause two groups to emerge and recombine [1]. Applications of this relatively recent technology may include gravimetry, magnetometry, and precision measurement of physical constants [6].

1.3 Effects of Cooling and Laser Pulses

A Rubidium 85 atom interferometer can be modeled as a two level system, but it is important to understand why. The experiment utilizes the D2 transition, which is between the $5^2P_{3/2}$ and $5^2S_{1/2}$ states of the single valence electron in the atomic system. This transition has two possible ground state values of F, the total atomic angular momentum, and the actual experiment involves the $F = 2$ and $F = 3$ ground states (Figure 1.1). The atoms are cooled by the lasers at a frequency just below the transition frequency. Because there is a little bit of energy "missing," the kinetic energy of the atom is absorbed in order to make the transition happen. After some time, the atom emits a photon of energy $\hbar\omega_0$, carrying away that kinetic

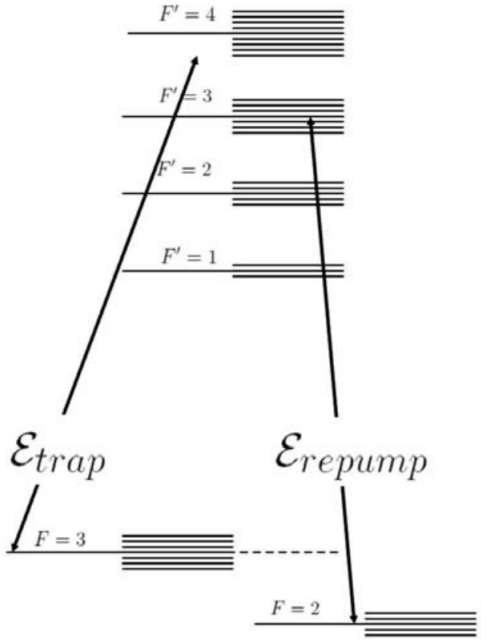

Figure 1.1. Relevant energy levels of the Rubidium 85 D2 transition. F is the total atomic angular momentum. Source: [1]

energy. As a result of this process, the atoms have less kinetic energy. Since this process happens nearly simultaneously to the whole group of atoms, the temperature of the group is lower. When this process is repeated, which can happen quite quickly in alkali atoms, dramatic cooling occurs on remarkably short timescales. The atoms in the experiment at the Naval Postgraduate School (NPS) start around 900K and cool very quickly to a few hundred μK. Complicating matters, however, some atoms undergoing this transition do not decay back into the $F = 3$ state, but instead go to the $F = 2$ state. In order to make these atoms useful for the experiment again, a second pumping laser at a different frequency is used to return these atoms back to the $F = 3$ state. Thus, the experiment requires two lasers, but this is only to cool the atoms to be used in the interferometer. Once the atoms are prepared in the proper F state, the interferometer deals with only one transition, and therefore the two level approximation is appropriate.

In the setup used by F. Narducci and others at NPS, laser cooling reduces the temperature of a group of Rubidium-85 atoms from room temperature to near absolute zero in a very short time scale. This reduces the noise caused by the velocity distribution of atoms at higher

temperatures, allowing for a more uniform experiment and precise measurement. Once these atoms are cooled, they are launched into freefall in a vertical vacuum chamber. A $\frac{\pi}{2}$ pulse excites half the atoms to a higher energy state and leaves half in the ground state, causing a split in phase space analogous to that produced by a beam splitter in optical interferometry. Next, after some amount of time T, a π pulse excites those atoms in the ground state and causes those in the excited state to fall back to the ground state. Finally, after another time T, a second $\frac{\pi}{2}$ pulse combines both groups of atoms. Half of the excited atoms are stimulated back to the ground state, and half of the ground state atoms jump to the excited state. The four possible paths converge into two paths at the end of the interferometer. Any phase differences due to gravitation, magnetic fields, or other sources of noise are measured at the end of this sequence.

Using the previous two level notation, the behavior of an atom in an interferometer starts in the $|0\rangle$ state. After the first $\pi/2$ pulse, the state of the atom is [4]

$$|\psi\rangle = \frac{1}{\sqrt{2}}\left(|0\rangle + |1\rangle\right) \tag{1.5}$$

The π pulse causes the $|0\rangle$ and $|1\rangle$ to switch places, although the overall state remains the same absent any phase factors picked up from external fields. More rigorously, we can say that for a time T after the first $\frac{\pi}{2}$ pulse, the state is

$$|\psi\rangle = \frac{1}{\sqrt{2}}(|0\rangle + e^{i\Theta_1 T}\,|1\rangle\,, \tag{1.6}$$

where $\Theta_1 T$ is a phase picked up due to some external field over time T. After the π pulse, the state becomes

$$|\psi\rangle = \frac{1}{\sqrt{2}}(|1\rangle + e^{i\Theta_1 T}\,|0\rangle), \tag{1.7}$$

and after another time T, the excited state again picks up a phase:

$$|\psi\rangle = \frac{1}{\sqrt{2}}(e^{i\Theta_2 T}\,|1\rangle + e^{i\Theta_1 T}\,|0\rangle). \tag{1.8}$$

Finally, after the last $\frac{\pi}{2}$ pulse, the state becomes

$$|\psi\rangle = \frac{1}{\sqrt{2}}\left[e^{i\Theta_2 T}\frac{1}{\sqrt{2}}\left(|0\rangle + |1\rangle\right) + e^{i\Theta_1 T}\frac{1}{\sqrt{2}}\left(|0\rangle + |1\rangle\right)\right], \tag{1.9}$$

where an extra factor of $\frac{1}{\sqrt{2}}$ comes from Equation 1.6. Usually the excited state is detected, so we find the excited state probability

$$|\langle 1|\psi\rangle|^2 = \frac{1}{4}\left(1 + e^{iT(\Theta_2-\Theta_1)} + e^{iT(\Theta_1-\Theta_2)} + 1\right). \tag{1.10}$$

The exponential terms reduce to $2\cos\Theta_2 - \Theta_1$. This Θ dependence is what makes the interferometer work. In the case when $\Theta_1 = \Theta_2$, we have a probability of 1 that the atom is in state $|1\rangle$ when the interferometer paths close, which is exactly what we would expect.

CHAPTER 2:
Wigner Distributions

The physics of atom interferometry is relatively simple: the Schrodinger equation applies, as with all quantum systems, and the Hamiltonian is relatively straightforward, involving neutral atoms, a gravitational field, any additional magnetic fields involved in the experimental setup, and the laser pulses. All these situations (with the curious exception of the gravitational field) are well examined in introductory quantum mechanics textbooks, and so the time evolution of the position, energy, and momentum of the atoms in the different paths are available. However, this paper uses a slightly different method than the traditional Schrodinger picture—that of the Wigner distribution—to help visualize what actually happens in the interferometer.

2.1 Wigner Distributions

The Wigner distribution is physically equivalent to the wave function used in the Schrodinger picture [7]. However, its advantage lies in simultaneously accounting for the position and momentum of the atoms. Given a wave function in position space $\psi(x)$, the Wigner distribution of this system can be found using the following formula [8]:

$$W(x,p) = \frac{1}{h}\int e^{-ipy/\hbar}\psi(x+y/2)\psi^*(x-y/2)dy \tag{2.1}$$

Similarly, given a function's wave function in momentum space $\phi(p)$, the Wigner distribution can be calculated by

$$W(x,p) = \frac{1}{h}\int e^{ixy/\hbar}\phi(p-y/2)\phi^*(p+y/2)dy \tag{2.2}$$

These equations are analogous to the time independent formulation of the Schrodinger equation. The time dependence of the Wigner distribution will be discussed in the next section, but for now we note ψ or ϕ can be time dependent. The Wigner distribution is not strictly speaking a probability distribution, but a probability amplitude, although the next section will show the relative ease with which a probability distribution can be obtained.

Notably, it can take on negative values, and it does quite often in the case of systems that are nonclassical [9]. Nevertheless, by using the Wigner distribution, the physics of atom interferometry can be shown quite clearly: atoms with the same momenta but different positions can be easily distinguished, and vice versa.

2.2 The Weyl Transform

The Wigner distribution is a special case of a mathematical construct called the Weyl transform. Applied to a generic operator $\hat{A}$, the Weyl transform $\tilde{A}$ is defined as [9]

$$\tilde{A}(x,p) = \int e^{-ipy/\hbar} \langle x + y/2| \hat{A} |x - y/2\rangle dy \tag{2.3}$$

Alternatively, the Weyl transform can be found by

$$\tilde{A}(x,p) = \int e^{ixy/\hbar} \langle p + y/2| \hat{A} |p - y/2\rangle dy \tag{2.4}$$

The Weyl Transform is largely beyond the scope of this paper, but it is mentioned here in order to point out that the Wigner distribution/Weyl transform system is a robust method of describing quantum mechanical processes entirely equivalent to the Schrodinger Equation. Thus, its utility and applications range far beyond the scale of this simple analysis.

Given these equations, if we calculate the Weyl transform of the density operator, defined as $\hat{\rho} = |\psi\rangle \langle\psi|$, we get

$$\tilde{A}(x,p) = \int e^{-ipy/\hbar} \langle x + y/2|\psi\rangle \langle\psi|x - y/2\rangle dy \tag{2.5}$$

which is identical to Equation 2.1, showing us that the Wigner distribution is the Weyl transform of the density operator.

We can also recover a probability distribution in one variable by integrating the Wigner distribution over the other variable. For example, if we integrate the Wigner distribution W with respect to momentum

$$\int W(x,p)dp = \frac{1}{h} \int \int e^{-ipy/\hbar} \psi(x + y/2)\psi^*(x - y/2)dydp, \tag{2.6}$$

we use the fact that $\int e^{ipy/\hbar}dp = h\delta(y)$, where $\delta(y)$ is the Dirac delta function, simplifies the formula to

$$\int W(x,p)dp = \psi^*(x)\psi(x) = |\psi(x)|^2. \tag{2.7}$$

Similarly, integrating over x leads us to the momentum probability distribution:

$$\int W(x,p)dx = \phi^*(p)\phi(p) = |\phi(p)|^2. \tag{2.8}$$

Furthermore, since we know from the Schrodinger picture of quantum mechanics that the expectation value of an operator is the integral of the probability density times the operator, the Wigner distribution can be integrated with an operator's Weyl transform to calculate the expectation value of the operator:

$$\langle A\rangle = \int\int W(x,p)\tilde{A}(x,p)dxdp \tag{2.9}$$

These formulas become very simple when the operator $\hat{A}$ in question is a function of $\hat{x}$ or $\hat{p}$ only, that is, when the commutation relation between position and momentum does not come into play. In these cases, the Weyl transform simply changes $\hat{x}$ to x and $\hat{p}$ to p. Some common expectation values follow:

$$\langle x\rangle = \int\int W(x,p)xdxdp \tag{2.10}$$

$$\langle p\rangle = \int\int W(x,p)pdxdp \tag{2.11}$$

$$\langle H\rangle = \int\int W(x,p)H(x,p)dxdp, \tag{2.12}$$

where $\langle H\rangle$ is the expectation value of the Hamiltonian, given by the operator $\hat{H} = \frac{\hbar^2}{2m}\frac{\partial^2}{\partial x^2} + V$.

2.3 Time Evolution of the Wigner Distribution

The time evolution of the Wigner distribution obeys the quantum Liouville equation [10]. To show this, we start with the time dependent Schrodinger equation, following the derivation in [9]:

$$\hat{H}\Psi(x,t) = i\hbar\frac{\partial\Psi(x,t)}{\partial t} \tag{2.13}$$

and the time derivative of equation 2.1:

$$\frac{\partial W}{\partial t} = \frac{1}{h}\int \frac{\partial}{\partial t}e^{-ipy/\hbar}\Psi(x+y/2,t)\Psi^*(x-y/2,t)dy. \tag{2.14}$$

We note that the exponential term in the integral is not time dependent, and so the time derivative involves a product rule for the ψ terms:

$$\frac{\partial W}{\partial t} = \frac{1}{h}\int e^{-ipy/\hbar}\left(\frac{\partial\Psi(x+y/2,t)}{\partial t}\Psi^*(x-y/2,t) + \frac{\partial\Psi^*(x-y/2,t)}{\partial t}\Psi(x+y/2,t)\right)dy. \tag{2.15}$$

From here, we use the Schrodinger equation to replace the time derivatives:

$$\frac{\partial\Psi(x,t)}{\partial t} = \frac{\hbar}{2im}\frac{\partial^2\Psi(x,t)}{\partial x^2} + \frac{1}{i\hbar}V\Psi(x,t). \tag{2.16}$$

Once this substitution is made, it is helpful to separate the integral into two different integrals. We collect all the terms that include the two spatial derivatives and call these kinetic terms, and the others involving V are the potential terms:

$$\frac{\partial W}{\partial t} = \frac{\partial W_T}{\partial t} + \frac{\partial W_V}{\partial t}. \tag{2.17}$$

We note here that two derivatives in x can be changed easily into one derivative each in x and y using the relation [9]

$$\frac{\partial^2}{\partial x^2}\Psi(x+y/2,t) = 2\frac{\partial}{\partial x}\frac{\partial}{\partial y}\Psi(x+y/2,t). \tag{2.18}$$

Doing so gives us a kinetic integral in y of an argument that has a y derivative in it:

$$\frac{\partial W}{\partial t} = \frac{1}{2\pi i m}\int e^{-ipy/\hbar}\left(\frac{\partial}{\partial x}\frac{\partial}{\partial y}\Psi(x+y/2,t)\right)\Psi(x-y/2,t) \\ - e^{-ipy/\hbar}\left(\frac{\partial}{\partial x}\frac{\partial}{\partial y}\Psi(x-y/2,t)\right)\Psi(x+y/2,t)dy. \tag{2.19}$$

Integration of both terms by parts yields

$$\frac{\partial W_T}{\partial t} = -\frac{p}{hm}\frac{\partial}{\partial x}\int e^{-ipy/\hbar}\Psi(x+y/2,t)\Psi^*(x-y/2,t)dy, \tag{2.20}$$

which reduces to

$$\frac{\partial W_T}{\partial t} = -\frac{p}{m}\frac{\partial W}{\partial x}. \tag{2.21}$$

We note here that the term $-\frac{p}{m} = -\frac{\partial H}{\partial p}$ from Hamilton's equations of classical mechanics.

Finding the potential terms of $\frac{dW}{dt}$ is a little simpler. Using the potential term of Equation 2.16 in Equation 2.15, we find

$$\frac{\partial W_V}{\partial t} = \frac{2\pi}{ih^2}\int e^{-ipy/\hbar}\left[V(x+y/2) - V(x-y/2)\right]\Psi(x+y/2,t)\Psi^*(x-y/2,t)dy. \tag{2.22}$$

We now use a power series expansion of the potential $V(x)$ in x to write

$$V(x+y/2) - V(x-y/2) = \sum_{l=0}^{\infty}\frac{1}{l!}\frac{\partial^l V}{\partial x^l}\left(\left(-\frac{1}{2}y\right)^l - \left(\frac{1}{2}y\right)^l\right). \tag{2.23}$$

All even powers of l equal zero in this expansion, so we rewrite this as

$$V(x+y/2) - V(x-y/2) = \sum_{l=0}^{\infty}\frac{1}{(2l+1)!}\frac{1}{2}^{2l}\frac{\partial^{2l+1}V}{\partial x^{2l+1}}y^{2l+1}. \tag{2.24}$$

Using Equation 2.24 in Equation 2.22, we note that each multiple of y can be scaled as a derivative of W with respect to p. When we combine this with our kinetic term, we get the following:

$$\frac{\partial W}{\partial t} = \sum_{l=0}^{\infty} \frac{(i\hbar/2)^{2l}}{(2l+1)!} \left(\frac{\partial W}{\partial p}\frac{\partial H}{\partial x} - \frac{\partial H}{\partial p}\frac{\partial W}{\partial x} \right)^{2l+1}. \tag{2.25}$$

If we assume that the potential is at most quadratic in x, then all terms higher than $l = 0$ disappear from the series. This equation reduces to an analogue of the classical Liouville equation:

$$\frac{\partial W}{\partial t} = \frac{\partial W}{\partial p}\frac{\partial H}{\partial x} - \frac{\partial H}{\partial p}\frac{\partial W}{\partial x}. \tag{2.26}$$

This is a key result because solutions to the Liouville equation allow the classical Hamilton equations of motion $x(t)$ and $p(t)$ to be used for the variables x and p in $W(x, p, t)$. Thus, the time evolution of a Wigner distribution of a given quantum system does not require the calculation of a new Wigner distribution using a corresponding change in the wave function.

2.4 Example: The Harmonic Oscillator

The quantum harmonic oscillator with potential $V(x) = \frac{1}{2}kx^2$, where k is the harmonic oscillator spring constant, is an excellent example of the utility of the Wigner distribution in illuminating important results that may not be as clear in the Schrodinger picture. The quantum harmonic oscillator has a ground state wave function [11]

$$\psi_0(x) = \frac{1}{\sqrt{a\sqrt{\pi}}} \exp\left\{ -\frac{x^2}{2a^2} \right\}, \tag{2.27}$$

where $a = \sqrt{\frac{\hbar}{m\omega}}$, m is the mass of the particle in the harmonic oscillator, and $\omega = \sqrt{\frac{k}{m}}$. To calculate the Wigner distribution (Figure 2.1), we use Equation 2.1 to obtain

$$W(x, p) = \frac{2}{h} \exp\left\{ \frac{-p^2a^2}{\hbar^2} - \frac{x^2}{a^2} \right\}. \tag{2.28}$$

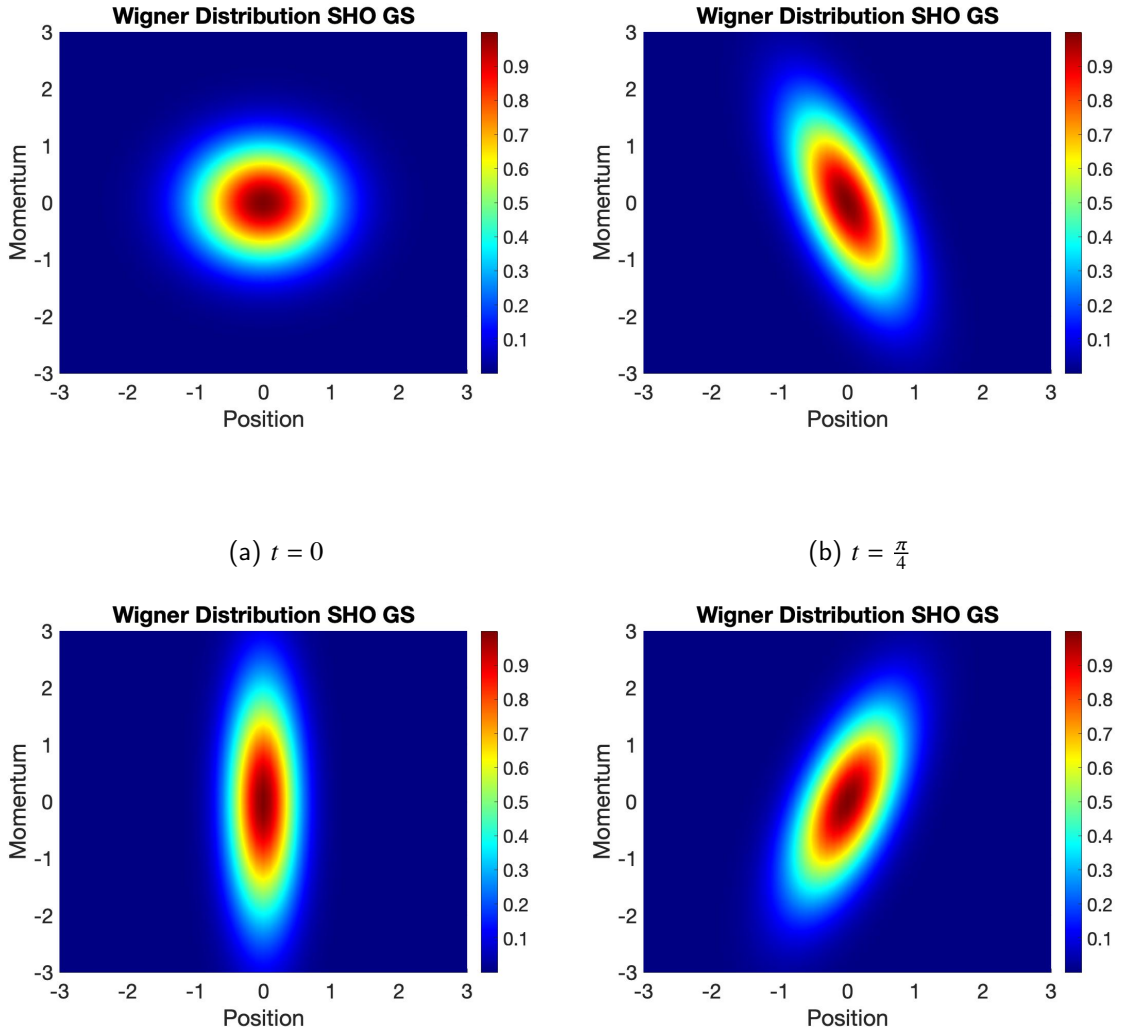

(a) $t = 0$

(b) $t = \frac{\pi}{4}$

(c) $t = \frac{\pi}{2}$

(d) $t = \frac{3\pi}{4}$

Figure 2.1. Wigner distribution of the ground state of the simple harmonic oscillator at four different times corresponding to one half period. The distribution is centered at $(x, p) = (0, 0)$. The coordinates of both axes are normalized.

To describe the time evolution of this Wigner distribution, we use the classical Hamiltonian

equations of motion for the harmonic oscillator:

$$x(t) = x_0 \cos(\omega t) - \frac{p_0}{m\omega} \sin(\omega t) \tag{2.29a}$$

$$p(t) = p_0 \cos(\omega t) + m\omega x_0 \sin(\omega t) \tag{2.29b}$$

where x_0 and p_0 are the position and momentum at time $t = 0$. The Wigner distribution then becomes

$$W(x, p, t) = \frac{2}{h} \exp\left\{ \frac{-a^2 (p_0 \cos(\omega t) + m\omega x_0 \sin(\omega t))^2}{\hbar^2} - \frac{(x_0 \cos(\omega t) - \frac{p_0}{m\omega} \sin(\omega t))^2}{a^2} \right\} \tag{2.30}$$

The above equation represents a distribution about $x = p = 0$, and is shown in Figure 2.1 for four different times. In order to center the distribution's motion at an arbitrary origin e.g. $(x = b, p = c)$, the offsets b and c can be added as initial conditions to the Hamilton equations of motion and substituted into the Wigner distribution from there:

$$x(t) = x_0 \cos(\omega t) - \frac{p_0}{m\omega} \sin(\omega t) - b \tag{2.31}$$

$$p(t) = p_0 \cos(\omega t) + m\omega x_0 \sin(\omega t) - c \tag{2.32}$$

The uncertainty in the ground state is minimal because the momentum is multiplied by a in the exponent while the position is divided by a. Therefore, the uncertainty relation remains independent of a, and is, in fact, $\hbar/2$. In excited states of the quantum harmonic oscillator, the uncertainty begins to grow [11].

2.5 Coherent and Squeezed States

However, there exist states known as coherent states which preserve this minimal uncertainty relation. These states are not eigenstates of the Hamiltonian, but are eigenstates of the annihilation or lowering operator $\hat{a}_- = \frac{1}{\sqrt{2\omega}} (-i\hat{p} + m\omega\hat{x})$. These states not only maintain minimum uncertainty, but their phase space propagation looks the most similar to a classical harmonic oscillator. This can be seen in Figure 2.2 where the state moves back and forth in

x and up and down in p, which is much different than the time evolution in Figure 2.1.

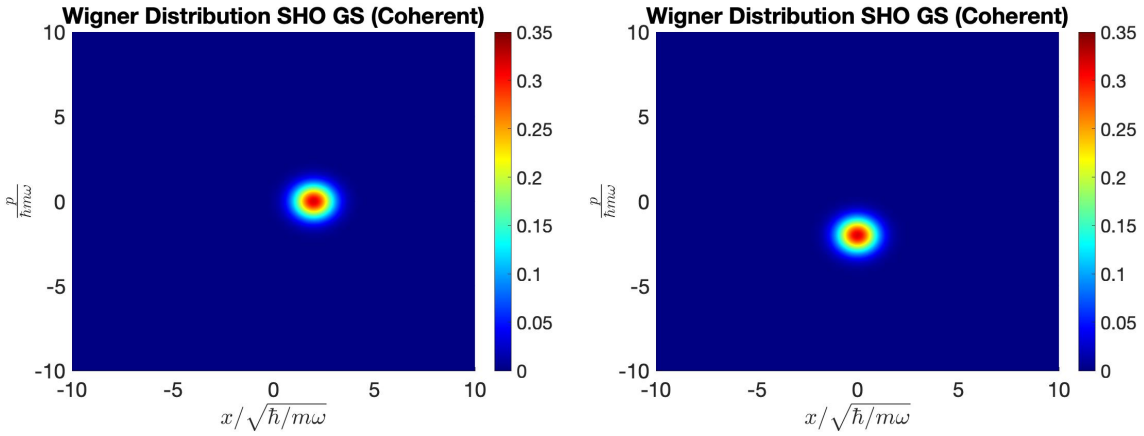

(a) $t = 0$

(b) $t = \frac{\pi}{2}$

(c) $t = \pi$

(d) $t = \frac{3\pi}{2}$

Figure 2.2. Time evolution of the Wigner distribution of a coherent state of the simple harmonic oscillator. Initially, the system is centered on $x = 2$ and $p = 0$. The distribution is symmetrical in position and momentum, and its time evolution traces a circle in phase space.

Furthermore, one of the more recent discoveries in optics is that of squeezed states [12], which are modifications of coherent states. Squeezed states achieve extremely small uncertainty in one variable by allowing for increased spreading in another. Thus, a coherent state

circular phase space distribution of position and momentum "squeezes" into an ellipse for a squeezed state. This can be accomplished by varying the value of a. Figure 2.3 shows the squeezed state Wigner distribution over one period of simple harmonic motion.

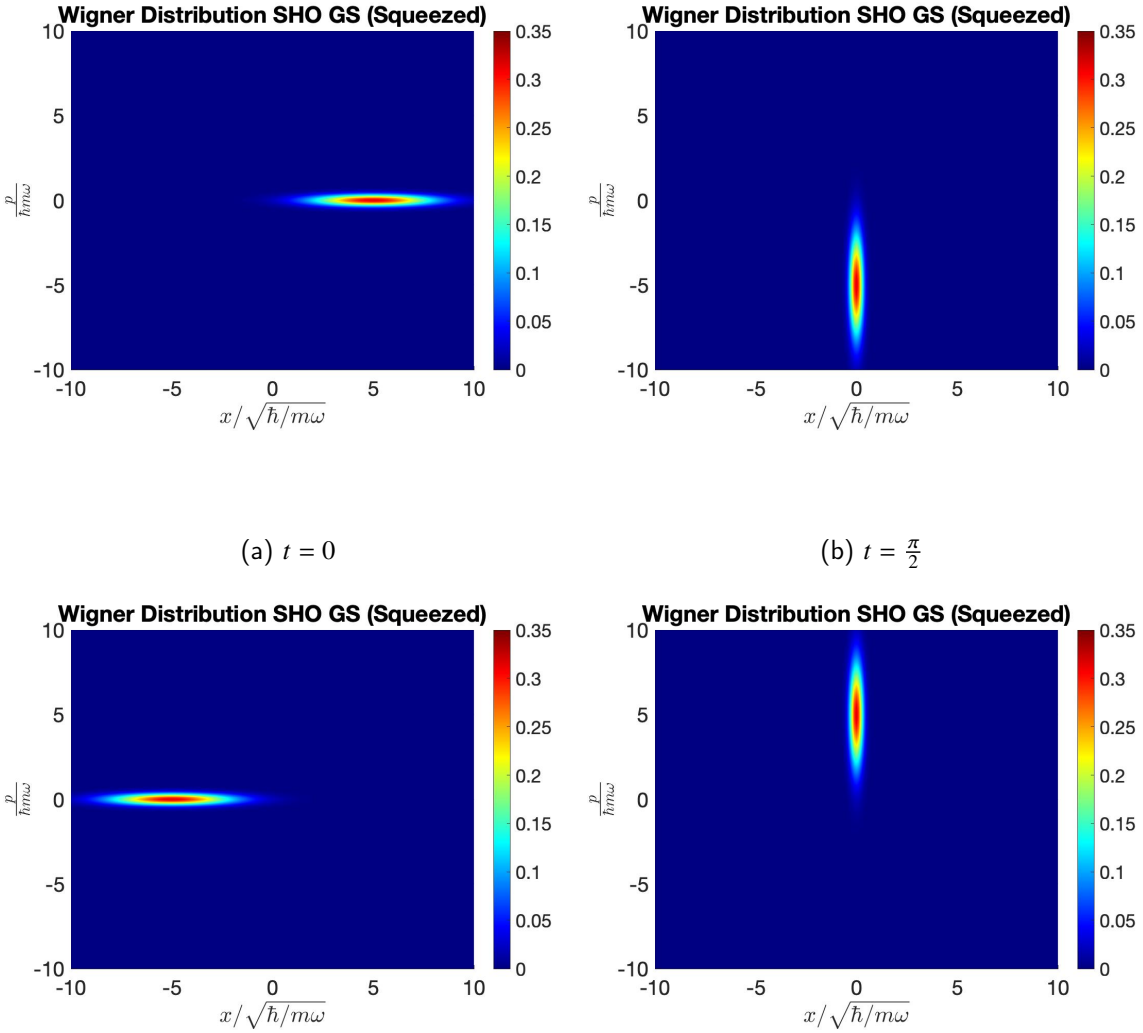

(a) $t = 0$

(b) $t = \frac{\pi}{2}$

(c) $t = \pi$

(d) $t = \frac{3\pi}{2}$

Figure 2.3. Squeezed ground state of the simple harmonic oscillator, for $a = 3\sqrt{\frac{\hbar}{m\omega}}$. Note that minimal total uncertainty is maintained throughout the period, although the distribution is much narrower in one parameter and wider in the other.

THIS PAGE INTENTIONALLY LEFT BLANK

CHAPTER 3:
Gravitational Fields

Having established the fundamentals of the Wigner distribution and atom interferometry, we now move towards our model, starting with the physics of gravity. The classical physics of gravitation are some of the first problems attempted in introductory physics classes. A particle starting at (vertical) position z_0 with initial velocity v_0 at time t_0 will propagate over time t as

$$z(t) = z_0 + v_0(t - t_0) + \frac{1}{2}g(t - t_0)^2, \tag{3.1}$$

where g is the constant of gravitational acceleration. However, as the length scale gets smaller, quantum mechanics start to dominate, and these problems are more complicated.

3.1 Quantum Mechanics of Free Particles

The mechanics of a particle in a gravitational potential are not ubiquitously covered in introductory quantum mechanics courses, where infinite square well, harmonic oscillator, and hydrogen atom problems dominate. This is because the mechanics of a free particle, the simplest system in Newtonian mechanics, is relatively complicated in the quantum domain. The plane wave solution to the Schrodinger equation ψ for a free particle is not normalizable because there are (by definition) no limitations on the position or momentum of the particle [11]. Analogously, a particle in a gravitational field does not behave well either. As a result, even solving for the wave function, much less the Wigner distribution, is complicated.

The wave function of a free particle as it propagates is dependent on the initial state $\Psi(x, 0)$ of the function [13]. Because of the Heisenberg uncertainty principle, the energy is not well defined, and so there is not a single eigenfunction solution to the problem. By the equivalent of Fourier theory in quantum mechanics, the initial state must be an integral over states of various wave numbers. The state is an integral instead of a sum because the wave number, which is proportional to the momentum, is continuous.

$$\Psi(x, 0) = \frac{1}{\sqrt{2\pi}} \int_{-\infty}^{\infty} \phi(k) e^{ikx} dk \tag{3.2}$$

Once $\phi(k)$ is known, then $\Psi(x,t)$ can be found by solving the Schrodinger equation:

$$\Psi(x,t) = \frac{1}{\sqrt{2\pi}} \int_{-\infty}^{\infty} \phi(k) e^{i(kx - \frac{\hbar k^2}{2m}t)} dk \tag{3.3}$$

The Wigner distribution then follows from Equation 2.1. If we suppose the initial state $\Psi(x,0)$ to be a Gaussian wave packet with minimal uncertainty, then we get the following Wigner distribution for the free particle of width σ:

$$W(x,p,t) = \frac{1}{\pi\hbar} \exp\left\{ -\frac{(x - pt/m)^2}{\sigma^2} - \frac{2\sigma^2 p^2}{\hbar} \right\}. \tag{3.4}$$

3.2 Gravity

The mechanics of a particle in a gravitational field are similar to a free particle in that the wave function cannot be normalized because there are no bounds or quantization measures on the particle's energy. To find the wave function of the particle in a gravitational field, we start with the (time independent) Schrodinger equation with a gravitational potential:

$$\frac{-\hbar^2}{2m} \frac{\partial^2 \psi(x)}{\partial x^2} + mgx\psi(x) = E\psi(x) \tag{3.5}$$

Using the substitution

$$y = \left(\frac{2m^2 g}{\hbar^2} \right)^{\frac{1}{3}} \left(x - \frac{E}{mg} \right), \tag{3.6}$$

the equation takes the simplified form

$$\frac{\partial^2 \psi}{\partial y^2} - y\psi = 0. \tag{3.7}$$

This equation is known as the Airy differential equation, and the solutions are Airy functions [14]. These functions decay exponentially when x is positive, and when x is negative, they alternate like a sinusoid with increasing frequency as x becomes more negative. To find the Wigner distribution, we integrate again, and find that the Wigner distribution is also an Airy function [15]:

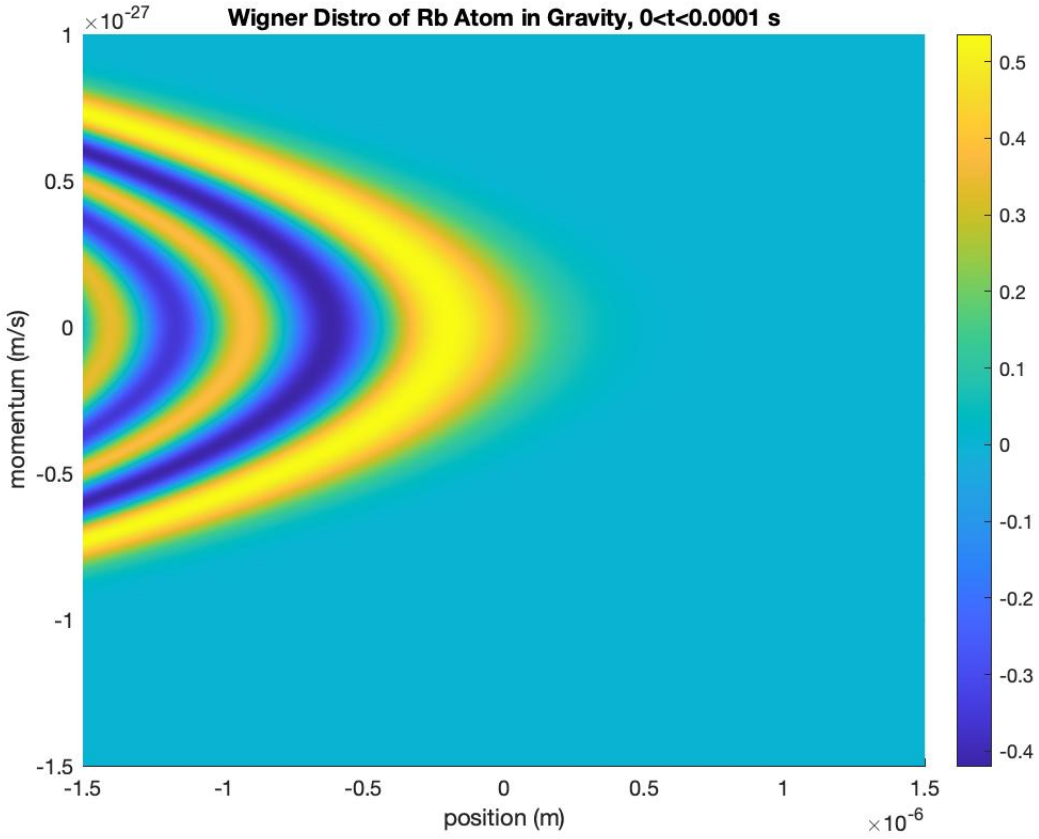

Figure 3.1. Wigner distribution at $t = 0$ and $E = 0$ for a Rubidium 85 atom in a gravitational field. Recall that the negative values imply a greater probability than those close to zero.

$$W(x,p) = N \cdot Ai\left[\left(\frac{8}{\hbar^2 m g^2}\right)^{1/3}\left(\frac{p^2}{2m} - mgx - E\right)\right] \tag{3.8}$$

where N is a normalization factor and E is the total energy of the system[1]. Figure 3.1 shows the graph of this Wigner distribution.

[1]For the full derivation of this formula, see E. Kajari, *Inertial and gravitational mass in quantum mechanics*

THIS PAGE INTENTIONALLY LEFT BLANK

CHAPTER 4:
Modeling Atom Interferometry

Although the gravitational field is in fact the potential through which atoms move in many atom interferometers, the Airy function modeling method does not take into account the initial velocity and position distributions of atoms produced by the laser cooling process. In this case, Rubidium 85 atoms are grouped together at low temperatures with Gaussian distributions in position and momentum, resulting in a Gaussian distribution in Wigner space. Because the Wigner distribution obeys the Liouville Equation (Equation 2.26), it is sufficient to use the classical dynamics of a gravitational system superimposed on the initial Wigner distribution of our choosing. As such, to actually model the atom interferometry, we will start with a Gaussian distribution in both velocity and position to model the state of the atoms when they are prepared for the interferometer by laser cooling.

4.1 Wigner Distribution of an Atom Interferometer

To model an atom interferometer, we start at time $t = 0$ with a Wigner distribution of a free particle in a Gaussian wave packet (Equation 3.4). We will then use the Hamilton equations of motion for a particle in a gravitational potential to allow the particles to propagate:

$$x(t) = x_0 + \frac{p}{m}(t - t_0) - \frac{1}{2}g(t - t_0)^2 \tag{4.1a}$$

$$p = p_0 - mg(t - t_0), \tag{4.1b}$$

which results in the following distribution:

$$W(x, p, t) = \frac{1}{\pi\hbar}\exp\left\{-\frac{(x - pt/m - \frac{1}{2}gt^2)^2}{\sigma^2} - \frac{2\sigma^2(p - mgt)^2}{\hbar}\right\}. \tag{4.2}$$

When this is done, Figure 4.1 shows the behavior of the distribution over time. The familiar arc of the parabola appears because of the gravitational acceleration, and the distribution's shape is otherwise maintained.

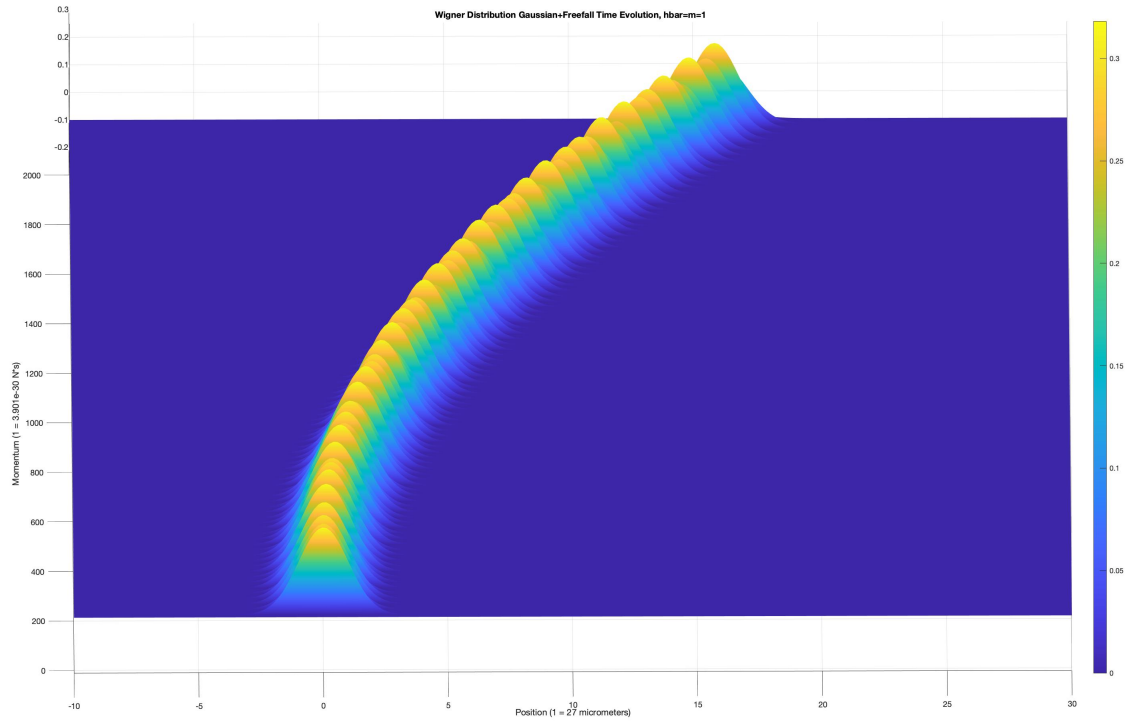

Figure 4.1. Time evolution of a Gaussian Wigner distribution of a Rubidium 85 atom in a gravitational field. Note that the dynamics of the distribution are entirely classical; quantum mechanics only factors into the initial shape of the distribution.

Adding the laser pulses to the model requires diligence. When a pulse excites an atom, the momentum changes immediately but the position does not. This is because we assume the laser pulses are delta functions in time that instantaneously change the momentum of the atoms. The new value of $\frac{p}{m}$ is integrated up to get a new position. If we start at time t_0 and apply our pulses at t_1, t_2, and t_3, each equally separated by time T, we obtain four different position and momentum functions, one for each of the possible phase space paths traveled in the interferometer:

$$x_1 = x_0 + \frac{1}{m}\left(p + p_{laser}\Theta(t - t_1) - p_{laser}\Theta(t - t_2) + p_{laser}\Theta(t - t_3)]\right) - \frac{1}{2}gt^2 \qquad (4.3a)$$

$$x_2 = x_0 + \frac{1}{m}\left(p + p_{laser}\Theta(t - t_1) - p_{laser}\Theta(t - t_2)\right)) - \frac{1}{2}gt^2 \tag{4.3b}$$

$$x_3 = x_0 + \frac{1}{m}\left(p + p_{laser}\Theta(t - t_2) - p_{laser}\Theta(t - t_3)\right)) - \frac{1}{2}gt^2 \tag{4.3c}$$

$$x_4 = x_0 + \frac{1}{m}\left(p + p_{laser}\Theta(t - t_2)\right)) - \frac{1}{2}gt^2 \tag{4.3d}$$

$$p_1 = p_0 - mgt + p_{laser}\Theta(t - t_1) - p_{laser}\Theta(t - t_2) + p_{laser}\Theta(t - t_3) \tag{4.4a}$$

$$p_2 = p_0 - mgt + p_{laser}\Theta(t - t_1) - p_{laser}\Theta(t - t_2) \tag{4.4b}$$

$$p_3 = p_0 - mgt + p_{laser}\Theta(t - t_2) - p_{laser}\Theta(t - t_3) \tag{4.4c}$$

$$p_4 = p_0 - mgt + p_{laser}\Theta(t - t_2) \tag{4.4d}$$

where $\Theta(t-t_n)$ is the Heaviside step function evaluated at time t and p_{laser} is the momentum added by the laser pulse.

It is important to confirm that the interferometer is closed, i.e. the paths result in the same final position and momentum when they converge. This convergence can be verified by substituting a time $t > t_3$ into the above equations. When this is done, paths 1 and 4 converge, as do paths 2 and 3. As a result, the paths of two different parabolas can clearly be seen in Figures 4.2a and 4.2b. Their combination is shown in Figure 4.3.

When we do these calculations again for a Rubidium 85 model with a laser wavelength of 780.24 nanometers, we obtain the simulation shown in Figures 4.4a, 4.4b, and 4.5. In these figures, the Gaussian functions that were initially represented as somewhat circular are far more elliptical in these graphs. The reason for this behavior is that the spreading in momentum is extremely small compared to the scale of the momentum change throughout the time evolution of the interferometer. This is a consequence both of the cooling of the atoms prior to their entrance into the interferometer and to the relatively large momentum changes that the Earth's gravity and the laser pulses provide. We will also model in the next section an interferometer in a harmonic oscillator potential.

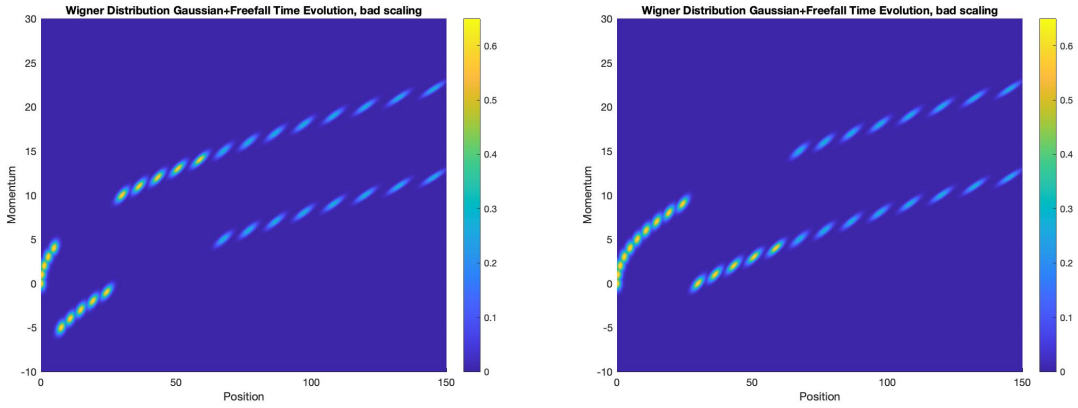

(a) Leg 1.

(b) Leg 2.

Figure 4.2. (a)Phase space path of two routes of an atom interferometer. The atom is excited by a $\pi/2$ pulse, relaxed by a π pulse, and excited agin by a $\pi/2$ pulse. Note: this is not to scale but merely illustrates the concept.(b)Phase space path of the other two routes of an atom interferometer. The atom is not excited by the initial $\pi/2$ pulse, then is excited by a π pulse, and the second $\pi/2$ pulse splits the path. Note: this graph is not to scale, the value of g, the gravitational acceleration, is far too low. These results could be reproduced if g was artificially lowered by a constant magnetic field in the opposite direction.

4.2 Modeling an Atom Interferometer in a Harmonic Oscillator Potential

To model an atom interferometer with atoms in a harmonic trap, we recall the harmonic oscillator equations of motion (Equations 2.31 and 2.29b) and the Wigner distribution (Equation 2.30). However, we will also need the Wigner distribution of an excited harmonic oscillator state. Using the first excited state wave function [11]

$$\psi_1(x) = \sqrt{\frac{2}{a\sqrt{\pi}}}\frac{x}{a}\exp\left\{-\frac{x^2}{2a^2}\right\} \tag{4.5}$$

we use equation 2.1 to integrate and find

$$W(x,p,t) = \frac{2}{h}\left(-1+2\left(\frac{ap}{\hbar}\right)^2+2\left(\frac{x}{a}\right)^2\right)\exp\left\{\left(x\cos(\omega t)-\frac{p}{m\omega}\sin(\omega t)\right)^2\right\} \tag{4.6}$$

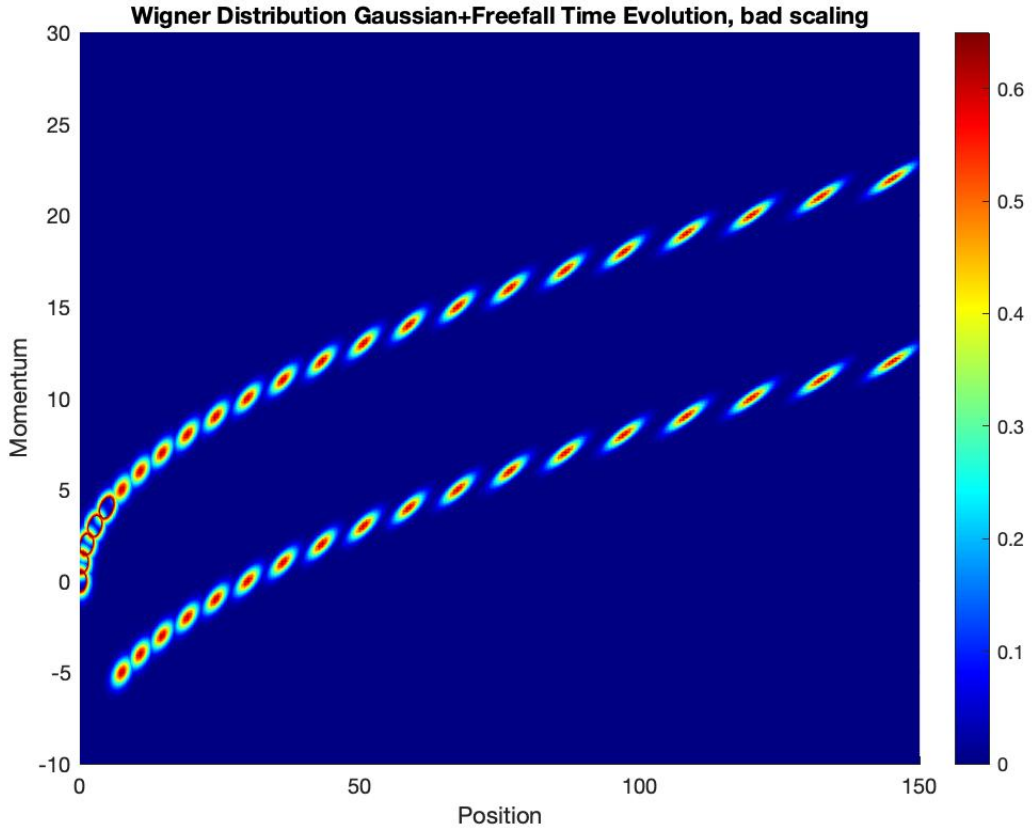

Figure 4.3. A full (improperly scaled) model of an atom interferometer. Note that after the initial $\pi/2$ pulse the subsequent pulses are indistinguishable. This shows that the interferometer is closed.

An interferometer that uses the ground state and first excited state of the quantum harmonic oscillator is very challenging to realize experimentally given the number of atoms and laser energy involved, but it is useful for showing quantum effects. Much like the gravitational potential model, the closed nature of the interferometer means that absent an inertial phase change or offset, the total state of the interferometer is consistently

$$W(x,p,t) = \frac{1}{2}(W_0(x,p,t) + W_1(x,p,t)), \tag{4.7}$$

as can be seen in Figure 4.6 The harmonic oscillator potential will produce the same results as the gravitational potential, but a potential advantage is that the momentum of the atoms

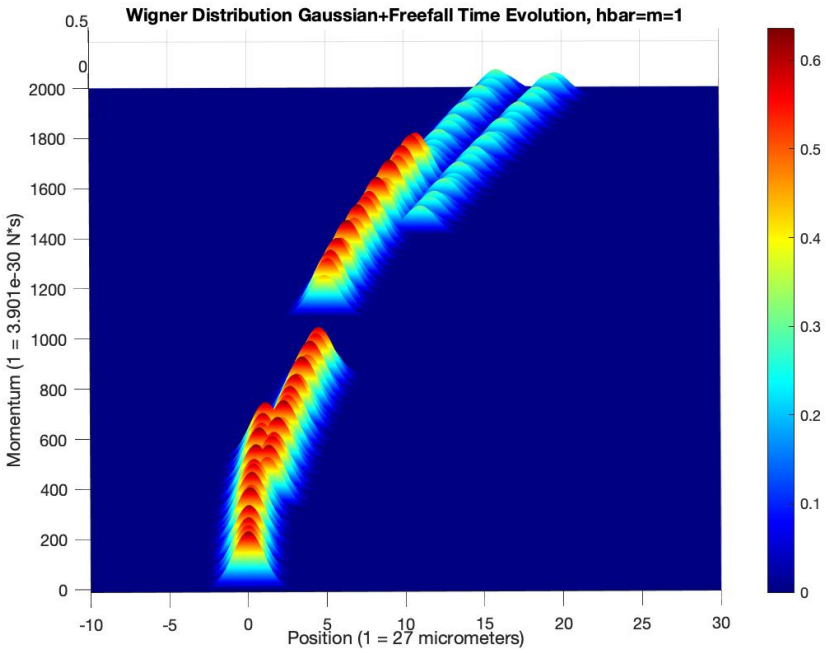

(a) Leg one.

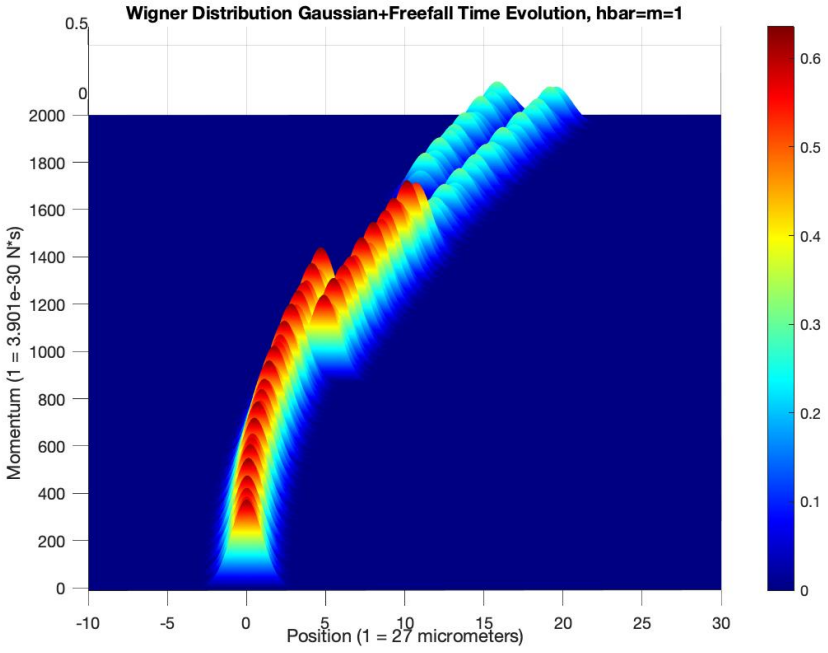

(b) Leg two.

Figure 4.4. The Wigner distribution of a Rubidium atom in an interferometer subject to a gravitational field. Figure a follows the path excited by the initial $\frac{\pi}{2}$ pulse, Figure b follows the path that remains in the ground state.

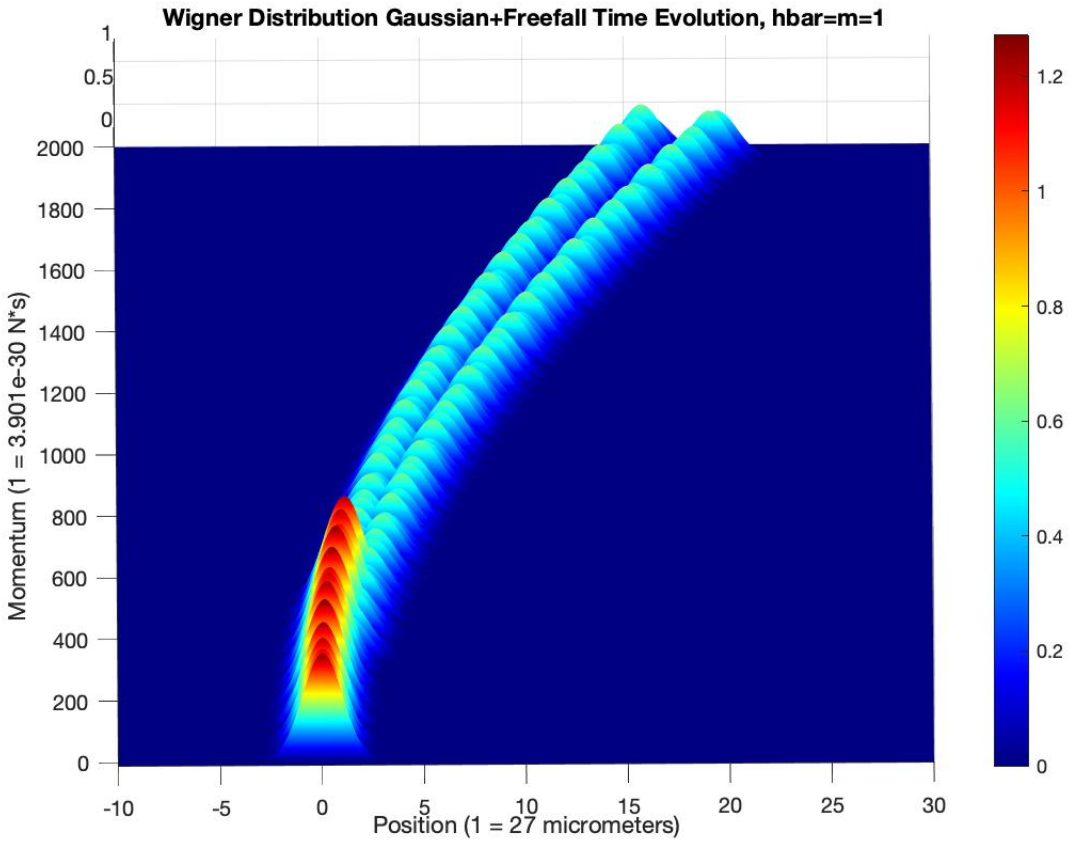

Figure 4.5. Wigner distribution of a Rubidium atom in an interferometer subject to a gravitational field. Because the laser pulses are perfect $\frac{\pi}{2}$ and π pulses, the two paths look identical even though there are two more pulses after the initial split.

is not increasing throughout the experiment. This could allow for better observation of the momentum axis of the Wigner distribution, as the large changes in momentum under the gravitational potential may obscure other aspects of the time evolution of the atom's momentum.

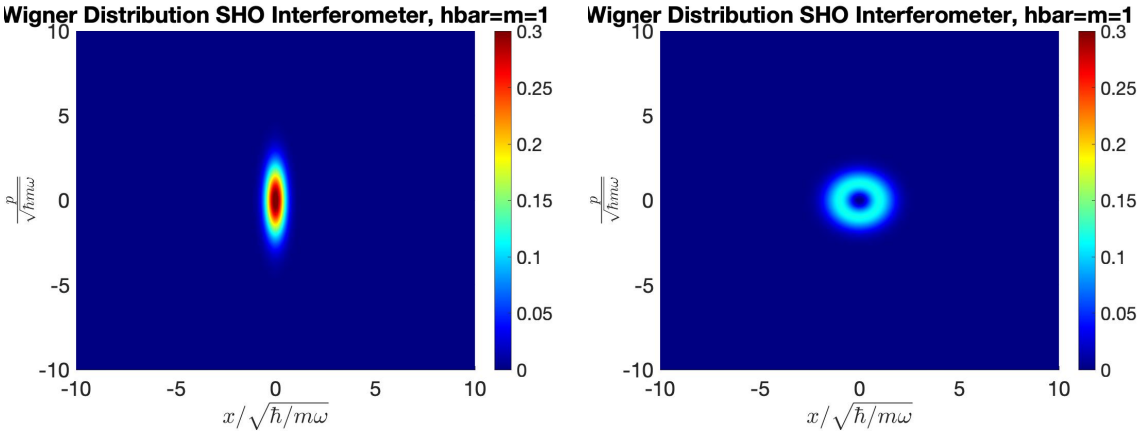

(a) $t = 0$

(b) $t = \frac{\pi}{2}$

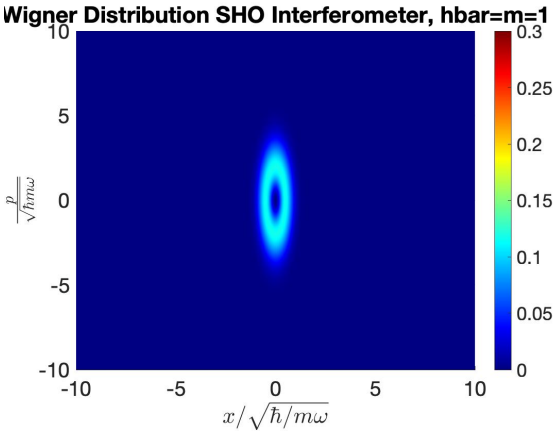

(c) $t = \pi$

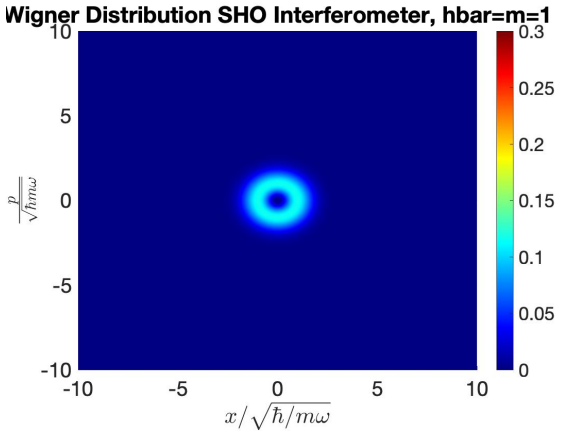

(d) $t = \frac{3\pi}{2}$

Figure 4.6. Wigner distribution of an atom interferometer in a harmonic oscillator potential. Note that the first $\frac{\pi}{2}$ pulse is between graphs a and b. The distribution is centered at $(x, p) = (0, 0)$.

CHAPTER 5:
Analysis, Further Work and Conclusion

Having modeled the behavior of an atom interferometer in two dimensions, we now turn to the significance of the experiment and possible results and applications that it can produce.

5.1 Why Wigner?

There was no absolute necessity to use the Wigner distribution to model the behavior of atoms in an interferometer. However, we chose it because of its ability to display the position and momentum distributions simultaneously. The Wigner distribution has a massive visual advantage over the traditional Schrodinger picture in the case of atom interferometry specifically. The laser pulses and their effects, which are not immediately apparent in position space, are instantly recognizable in Wigner space, as can be seen in Figure 4.5. Furthermore, the phase space distribution gives the viewer a more immediate grasp on the time evolution of the system. It is very hard to accurately observe changes in the position and velocity of a wave function at a glance, but the Wigner distribution transmits this information in way that is quite easily understood by someone without a formal background in physics.

The Wigner distribution is also a nice way to demonstrate the peculiarities of quantum mechanics. The Heisenberg uncertainty principle guarantees that the Wigner distribution will never be a point. This fact means that the shape of the distribution immediately gives information about the uncertainty in both parameters. In cases of minimal uncertainty, like the coherent and squeezed states of Figures 2.2 and 2.3, the shape of the Wigner distribution communicates the peculiarities of these states in a way that leaves little doubt about their behavior. In the Schrodinger picture, the graph would be nowhere near as clear. The purpose of these simulations was to attempt to find any previously unknown quantum effects that can affect the coherence of atom interferometers. Although these effects have not yet been found, further work could better establish the relationship between phase differences measured by the interferometer and how they appear when modeled with the Wigner distribution.

5.2 Further Work

The analysis done in this paper is a fairly broad and idealized general introduction to atom interferometers and their behavior seen through the lens of the Wigner distribution. Further work in modeling could be done by including a whole spread of atoms instead of just one in the model, adjusting external fields to produce phase differences, and in the case of the harmonic oscillator potential, adjusting the excited state parameters to a classical approximation. The production of phase differences could be done by modifying the time between pulses to slightly off the π and $\frac{\pi}{2}$ values divided by the Rabi frequency or changing the external potentials to values that are less uniform in space and/or time. These more precise models could then be contrasted to actual experimental data in order to determine the degree to which the experiment is behaving the way we expect.

5.3 Conclusion

Although atom interferometers are not yet widely used operationally, they are quite promising. The use of lasers to cool atoms to near absolute zero is fascinating in itself, and atom interferometry is but one important application of this technology. Plenty of variations in their path, pulse sequence, and shape are possible, and therefore this technology only looks to become more efficient, precise, and applicable over time. The Wigner distribution is also an excellent way to show what the atoms actually do inside the interferometer, and therefore it is a worthwhile analysis of this growing technology.

List of References

[1] S. A. D. F. A. Narducci, J. P. Davis, "A study of raman resonances in arbitrary magnetic fields using cold atoms," *NAVAIR Journal for Scientists and Engineers*, vol. 1, p. 12, July 1 July 2012.

[2] W. M. Macek and D. T. M. Davis, "Rotation rate sensing with traveling[U+2010]wave ring lasers," *Applied Physics Letters*, vol. 2, no. 3, pp. 67–68, 1963. Available: https://doi.org/10.1063/1.1753778

[3] L. Allen and J. H. Eberly, "Optical resonance and two-level atoms." Available: https://www.osti.gov/biblio/7365050

[4] M. O. Scully and M. S. Zubairy, *Quantum Optics*. Cambridge University Press, 1997.

[5] J. Davis and F. Narducci, "A proposal for a gradient magnetometer atom interferometer," *Journal of Modern Optics*, vol. 55, no. 19-20, pp. 3173–3185, nov 2008.

[6] S. Abend, M. Gersemann, C. Schubert, D. Schlippert, E. M. Rasel, M. Zimmermann, M. A. Efremov, A. Roura, F. A. Narducci, and W. P. Schleich, "Atom interferometry and its applications," 2020.

[7] T. Curtright, D. Fairlie, and C. Zachos, "Features of time-independent wigner functions," *Physical Review D*, vol. 58, no. 2, Jun 1998. Available: http://dx.doi.org/10.1103/PhysRevD.58.025002

[8] J. A. Poulsen, S. K.-M. Svensson, and G. Nyman, "Dynamics of gaussian wigner functions derived from a time-dependent variational principle," *AIP Advances*, vol. 7, no. 11, p. 115018, nov 2017.

[9] W. B. Case, "Wigner functions and weyl transforms for pedestrians," *American Journal of Physics*, vol. 76, no. 10, pp. 937–946, oct 2008.

[10] H. Bauke and N. R. Itzhak, "Visualizing quantum mechanics in phase space," 2011.

[11] D. J. Griffiths, *Introduction to Quantum Mechanics (2nd Edition)*, 2nd ed. Pearson Prentice Hall, Apr. 2004. Available: http://www.amazon.com/exec/obidos/redirect?tag=citeulike07-20&path=ASIN/0131118927

[12] R. Schnabel, "Squeezed states of light and their applications in laser interferometers," *Physics Reports*, vol. 684, p. 1–51, Apr 2017. Available: http://dx.doi.org/10.1016/j.physrep.2017.04.001

[13] W. Schleich, J. Dahl, and S. Varró, "Wigner function for a free particle in two dimensions: A tale of interference," *Optics Communications*, vol. 283, no. 5, pp. 786–789, mar 2010.

[14] N. Wheeler and R. C. P. Department, "Classical/quantum dynamics in a uniform gravitational field: A. unobstructed free fall," Tech. Rep. the, 2002.

[15] E. Kajari, N. L. Harshman, E. M. Rasel, S. Stenholm, G. Süßmann, and W. P. Schleich, "Inertial and gravitational mass in quantum mechanics," *Applied Physics B*, vol. 100, no. 1, p. 43–60, Jun 2010. Available: http://dx.doi.org/10.1007/s00340-010-4085-8

Initial Distribution List

1. Defense Technical Information Center
   Ft. Belvoir, Virginia

2. Dudley Knox Library
   Naval Postgraduate School
   Monterey, California